CHEMISTRY
A EUROPEAN JOURNAL

DOI: 10.1002/chem.200800044

New $M_3N@C_{2n}$ Endohedral Metallofullerene Families (M = Nd, Pr, Ce; n = 40–53): Expanding the Preferential Templating of the C_{88} Cage and Approaching the C_{96} Cage

Manuel N. Chaur,[a] Frederic Melin,[a] Bevan Elliott,[a] Amar Kumbhar,[b] Andreas J. Athans,[a] and Luis Echegoyen*[a]

Abstract: Three new families of trimetallic nitride template endohedral metallofullerenes (TNT EMFs), based on cerium, praseodymium, and neodymium clusters, were synthesized by vaporizing packed graphite rods in a conventional Krätschmer–Huffman arc reactor. Each of these families of metallofullerenes was identified and characterized by mass spectroscopy, HPLC, UV/Vis-NIR spectroscopy, and cyclic voltammetry. The mass spectra and HPLC chromatograms show that these larger metallic clusters are preferentially encapsulated by a C_{88} cage. When the size of the cluster is increased, the C_{96} cage is progressively favored over the predominant C_{88} cage. It is also observed that the smaller cages (C_{80}–C_{86}) almost disappear on going from neodymium to cerium endohedral metallofullerenes. The UV/Vis-NIR spectra and cyclic voltammograms confirm the low HOMO–LUMO gap and reversible electrochemistry of these $M_3N@C_{88}$ metallofullerenes.

Keywords: electrochemistry · HOMO–LUMO gap · HPLC · mass spectrometry · metallofullerenes · template synthesis

Introduction

Fullerenes that encapsulate a trimetallic nitride cluster are known as trimetallic nitride template endohedral metallofullerenes (TNT EMFs) and are usually synthesized by arcing graphite rods. The graphite rods are packed with a metal oxide and vaporized at low pressures in a Krätschmer–Huffman reactor in the presence of a nitrogen source. The first example of a TNT EMF, $Sc_3N@C_{80}$, was prepared by Dorn and co-workers in 1999.[1] Since its discovery, several fullerene-encapsulated metal-based nitride clusters[1–9] and mixed metal nitride endohedral fullerenes[1,10] have been successfully prepared and characterized. In each case, these compounds have a wide distribution of cage sizes, which range from cages as small as C_{68} to those as large as C_{98}.[8] However, as the size of the metallic cluster is increased, the yield of the EMFs decreases drastically, as in the case of the $Gd_3N@C_{2n}$ ($40 \le n \le 44$) family of EMFs,[6] which is formed in one of the lowest yields for a synthesized EMF when compared with other metallofullerenes with smaller metallic clusters.[8,4]

As a result of their structures and electronic properties, EMFs are unique compounds that have potential applications in several different fields, such as in molecular electronics and as contrast agents in magnetic resonance imaging.[11,12]

Until recently, all of the isolated EMFs had a common characteristic, that is, the preferential templating of C_{80} cages. This is favored for most metallic clusters owing to an electronic stabilization between the metallic cluster and the fullerene cage,[13] which gives $M_3N@C_{80}$ (M = metal) as the most abundant species in the fullerene soot after the arcing process. Recently our group reported an $Nd_3N@C_{2n}$ EMF[14] that showed for the first time preferential templating of a larger cage (C_{88}), which was probably the result of both the size and the electronic stabilization of the cluster. This result

[a] M. N. Chaur, Dr. F. Melin, B. Elliott, Dr. A. J. Athans, Prof. Dr. L. Echegoyen
Chemistry Department, Clemson University
219 Hunter Laboratories, Clemson, SC 29630-0973 (USA)
Fax: (1+)864-656-6613
E-mail: luis@clemson.edu

[b] A. Kumbhar
Advanced Materials Research Laboratories
91 Technology Dr., Anderson, SC 29625 (USA)

Supporting information for this article is available on the WWW under http://www.chemeurj.org/ or from the author.

prompted the question of whether a C_{88} cage is the maximum size limit for metallofullerenes or if larger clusters would favor still larger cages, and if so, which cages would those be?

Another interesting property of EMFs is that their electrochemical behavior changes dramatically as the cage size increases. It was recently observed that as the cage size increased from C_{80} to C_{88}, the reduction waves became completely reversible and the HOMO–LUMO gap decreased considerably.[14,15]

Herein we report the synthesis and isolation of Nd-, Pr-, and Ce-based EMFs and their characterization by mass spectrometry, HPLC, UV/Vis-NIR spectroscopy, and cyclic voltammetry. These three families of TNT EMFs are the largest to be isolated to date and all present the same preferential C_{88} templating. In addition, the C_{96} cage is increasingly favored as the metal size is increased.

Results and Discussion

Synthesis and identification of the $M_3N@C_{2n}$ (M=Nd, Pr, Ce) EMF families: The families of EMFs were synthesized in a conventional Krätschmer–Huffman arc reactor. Graphite rods were packed with a mixture of the corresponding metal oxide and graphite powder and then burned in a He/NH_3 atmosphere. For the synthesis of $Nd_3N@C_{2n}$ ($40 \le n \le 50$) and $Pr_3N@C_{2n}$ ($40 \le n \le 52$), a 1:1 graphite/metal oxide mixture gave the highest yield of metallofullerenes (0.2 mg of fullerenes per rod for Nd and 0.4 mg of fullerenes per rod for Pr). For $Ce_3N@C_{2n}$ ($43 \le n \le 53$), the maximum yield of fullerenes (0.1 mg of fullerenes per rod) was obtained when the graphite rods were packed with a 3:1 mixture of graphite powder and cerium oxide.

Figure 1 shows the mass spectra and HPLC chromatograms of the $Nd_3N@C_{2n}$, $Pr_3N@C_{2n}$, and $Ce_3N@C_{2n}$ families. From the mass spectra it is evident that a wider range of EMF sizes was obtained as the size of the metal in the cluster was increased (Figure 1a) and metallofullerenes with cages as large as C_{106} were formed (Figure 1a, bottom). Both the Nd and Pr species gave a very low amount of the C_{80} metallofullerene, and no C_{82} metallofullerene was observed. In the case of $Ce_3N@C_{2n}$, only a small amount of the C_{86} metallofullerene was formed. The mass spectra and HPLC chromatograms also show the formation of two monometallofullerenes under these arcing conditions, $Pr@C_{84}$ (Figure 1, **y′**) and $Ce@C_{84}$ (Figure 1, **y″**) The yields of these monometallofullerenes were favored as the metal size was increased; for Ce, a relatively high abundance of this species was observed in the chromatogram, but for Nd no $Nd@C_{84}$ was observed.

The identity of each peak in the chromatogram was established by mass spectrometry and the products were isolated by using a one-stage HPLC separation. The purity was checked by using a two-stage HPLC separation with a linear combination of a Buckyprep-M and a Buckyprep column. No further purification was necessary. Energy dispersive spectroscopy (EDS) performed on some of the isolated samples showed the characteristic peaks of Nd, Pr and cerium (see the Supporting Information).

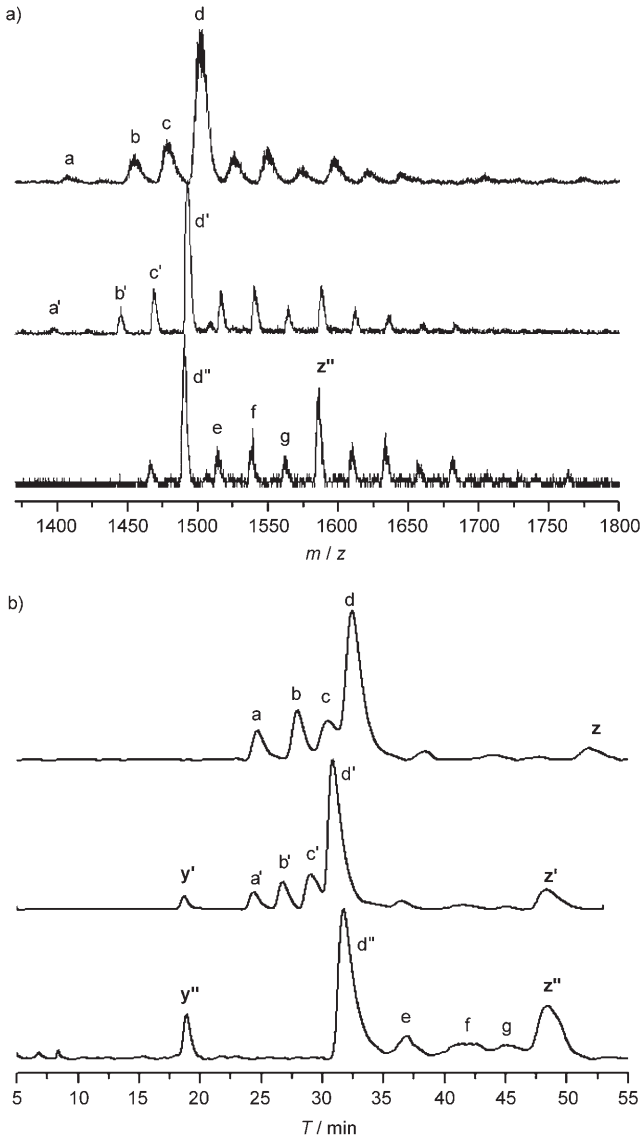

Figure 1. a) Mass spectra of the $Nd_3N@C_{2n}$ (top), $Pr_3N@C_{2n}$ (middle) and $Ce_3N@C_{2n}$ (bottom) EMF families. **z″** indicates the signal assigned to $Ce_3N@C_{96}$. b) HPLC chromatograms of the $Nd_3N@C_{2n}$ (top), $Pr_3N@C_{2n}$ (middle) and $Ce_3N@C_{2n}$ (bottom) EMF families. **y′**: $Pr@C_{84}$, **y″**: $Ce@C_{84}$, **z**: $Nd_3N@C_{96}$ **z′**: $Pr_3N@C_{96}$, and **z″**: $Ce_3N@C_{96}$. See text for the assignment of peaks **a**–**g**. Conditions: eluent = toluene, flow rate = 4.0 mL min^{-1}; Buckyprep-M column; detection wavelength = 372 nm.

$Nd_3N@C_{2n}$ ($40 \le n \le 50$) has four main fractions in its HPLC chromatogram, which were identified as $Nd_3N@C_{80}$ (**a**), $Nd_3N@C_{84}$ (**b**), $Nd_3N@C_{86}$ (**c**), and $Nd_3N@C_{88}$ (**d**) (see Figure 1b, top, and the Supporting Information), of which $Nd_3N@C_{88}$ was the most abundant species. Larger metallofullerenes were also observed, but in very low yields and with poor isomeric purity.

$Pr_3N@C_{2n}$ ($40 \le n \le 52$) showed a broader distribution of cage sizes than its Nd counterpart. The product contained a

significant amount of $Pr_3N@C_{96}$ (**z′**) and a lower concentration of metallofullerenes with cages smaller than C_{88}. $Pr_3N@C_{80}$ (**a′**) was produced in very low amounts. Peaks **b′** and **c′** were identified as $Pr_3N@C_{84}$ and $Pr_3N@C_{86}$, respectively (see Figure 1b, middle, and the Supporting Information).

The $Ce_3N@C_{2n}$ ($43 \leq n \leq 53$) EMF family mainly contained metallofullerenes larger than $Ce_3N@C_{86}$, in which $Ce_3N@C_{88}$ (**d″**) and $Ce_3N@C_{96}$ (**z″**) were the most abundant species. The other peaks (**e**–**g**) were identified as $Ce_3N@C_{90}$, $Ce_3N@C_{92}$, and $Ce_3N@C_{94}$, respectively; however, their isomeric purity is probably low because as the cage size increases, the number of possible isomeric structures also increases dramatically.[16] For example, there are 187 possible isomers that follow the isolated pentagon rule (IPR) for C_{96}, which explains why the purification process is a major issue in metallofullerene research. Recent computational work has shown that the number of isomeric IPR cages with an electronic structure that can accept the transfer of six electrons from the cluster is actually quite low,[17] but the presence of multiple isomers still cannot be ruled out.

Previously reported TNT EMFs have shown a preference for templating the C_{80} cage, but Nd_3N preferentially templates the C_{88} cage,[14] and the same preferential templating is reported herein for both Pr and Ce. As the size of the metal increased, a gradual increase in the abundance of the C_{96} cage was observed; both the mass spectra and HPLC chromatograms show that the abundance of the $M_3N@C_{96}$ (M = Nd, Pr, Ce) EMFs gradually increases to the point that $Ce_3N@C_{96}$ is the second most abundant species in the $Ce_3N@C_{2n}$ ($43 \leq n \leq 53$) family (see Figure 1). From these features, it would be expected that for an even bigger cluster (i.e., La_3N), a considerably higher amount of $M_3N@C_{96}$ would be found or that preferential templating of the C_{96} cage would be observed.

UV/Vis-NIR spectra of the isolated Nd-, Pr-, and Ce-based EMFs: It has been demonstrated that the electronic absorptions of metallofullerenes are due to π–π^* transitions of the fullerene cage.[2,18] It is also known that the spectral onset in the UV/Vis-NIR spectrum can be used to calculate the optical band gap.[19] Usually, 1.0 eV is used to differentiate between small and large band gap fullerenes,[2,19] so metallofullerenes with an optical band gap larger than 1.0 eV are considered to be large band gap EMFs, which determines their reactivity and stability to some degree.

The isolated EMFs were dissolved in toluene and their UV/Vis-NIR spectra were recorded. Figure 2 shows the electronic spectra of the isolated products of the Nd_3N and Pr_3N EMF families. Their corresponding absorption peaks, spectral onsets, and optical band gaps are listed in Table 1.

$Nd_3N@C_{80}$ and $Pr_3N@C_{80}$ both have a strong visible absorption at $\lambda = 404$ nm. Two other peaks were also observed in the same region, and all of these absorptions correlate well with the peaks observed for their $M_3N@C_{80}$ (I_h; M = Gd, Dy, Tm) counterparts, which suggests that they have similar electronic and structural properties. The HOMO–LUMO gaps were calculated to be 1.55 eV for $Nd_3N@C_{80}$ and 1.51 eV for $Pr_3N@C_{80}$. These values fall within the range of 1.50 to 1.60 eV that is usually calculated for metallofullerenes with the general formula $M_3N@C_{80}$ (M = Sc, Tb, Ho, Y, Er, Tm, Dy, Gd).[2,4,6,20]

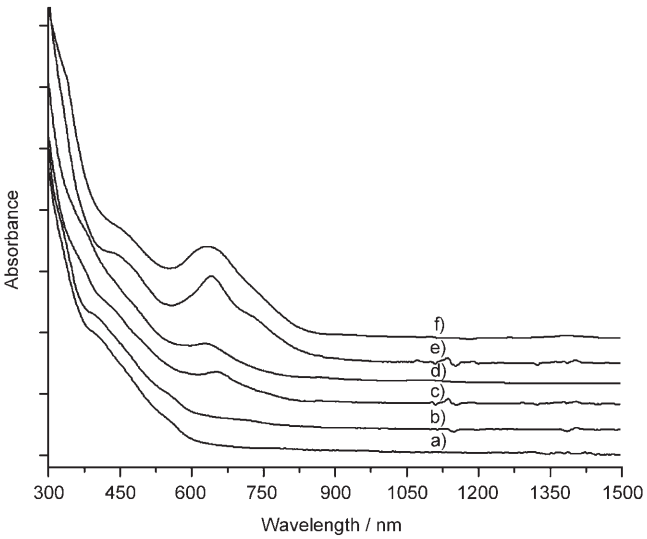

Figure 2. UV/Vis-NIR spectra of the $Nd_3N@C_{2n}$ and $Pr_3N@C_{2n}$ EMFs dissolved in toluene. a) $Nd_3N@C_{80}$, b) $Pr_3N@C_{80}$, c) $Nd_3N@C_{84}$, d) $Pr_3N@C_{84}$, e) $Nd_3N@C_{86}$, and f) $Pr_3N@C_{86}$

Table 1. Characteristic spectral onsets, band gaps and UV/Vis-NIR absorptions of some of the $M_3N@C_{2n}$ ($n = 40, 42, 44$) species.

	Onset [nm]	Band gap[a] [eV]	UV/Vis-NIR λ [nm]
$Nd_3N@C_{80}$	800	1.55	404, 560, 721
$Pr_3N@C_{80}$	820	1.51	404, 555, 728
$Nd_3N@C_{84}$	1041	1.19	358, 441, 655
$Pr_3N@C_{84}$	1342	0.92	380, 488, 627, 1086
$Nd_3N@C_{86}$	1194	1.04	338, 445, 641, 739
$Pr_3N@C_{86}$	1479	0.84	335, 461, 636, 744, 1389
$Nd_3N@C_{88}$	1420	0.87	390, 770, 965
$Pr_3N@C_{88}$	1445	0.86	395, 491, 775, 955
$Ce_3N@C_{88}$	1442	0.86	395, 481, 769, 949

[a] Band gap calculated from the spectral onset (band gap $\approx$ 1240 per onset).[8]

The spectrum of $Nd_3N@C_{84}$ shows a relatively smaller spectral onset and thus a higher optical band gap than $Pr_3N@C_{84}$ and other isolated $M_3N@C_{84}$ (M = Dy, Tb, Gd) metallofullerenes, and it can, therefore, be classified as a large-band gap metallofullerene. However, its absorption peaks resemble those observed for $Pr_3N@C_{84}$ and $Gd_3N@C_{84}$[15] with the exception of the NIR absorption, which is not present in the spectrum of $Nd_3N@C_{84}$. On the other hand, $Pr_3N@C_{84}$ has a band gap that is closer to that of $Gd_3N@C_{84}$, and some very close absorptions as well, such as the UV absorption at $\lambda = 380$ nm, two visible absorptions at $\lambda = 488$ and 627 nm, and finally a NIR absorption at $\lambda =$ 1086 nm.

$Nd_3N@C_{86}$ and $Pr_3N@C_{86}$ have very similar electronic spectra, but $Pr_3N@C_{86}$ has an additional absorption in the NIR region and its spectral onset is located at around $\lambda =$

1479 nm, which results in the same optical band gap as that reported for $Dy_3N@C_{86}$.[8]

The UV/Vis-NIR spectra of $Nd_3N@C_{88}$, $Pr_3N@C_{88}$, and $Ce_3N@C_{88}$ are quite similar, which suggests that these TNT EMFs share the same structure. A very strong absorption located between $\lambda = 769$ and 775 nm and NIR absorptions at around $\lambda = 949$ and 965 nm were found for all three metallofullerenes. $Nd_3N@C_{88}$ has an optical band gap of 0.87 eV, whereas for $Pr_3N@C_{88}$ and $Ce_3N@C_{88}$ the band gap is 0.86 eV (see Figure 3 and Table 1).

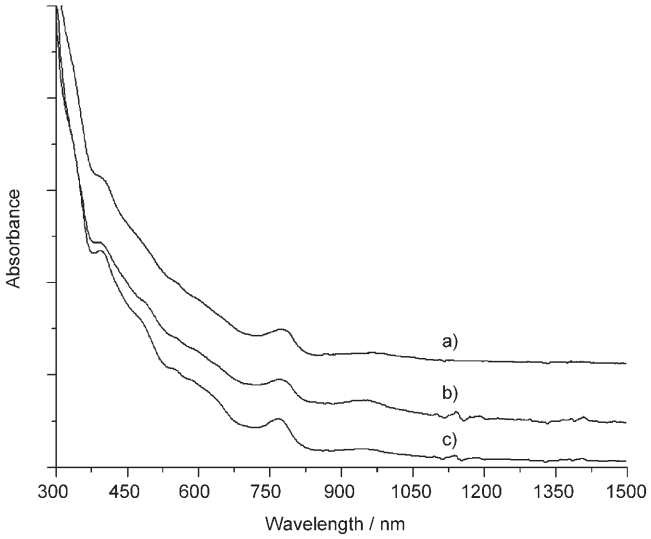

Figure 3. UV/Vis-NIR spectra of a) $Nd_3N@C_{88}$, b) $Pr_3N@C_{88}$, and c) $Ce_3N@C_{88}$ EMFs in toluene.

Electrochemical studies of the Nd, Pr, and Ce EMF families: The electrochemical studies were conducted in a 0.05 M solution of NBu_4PF_6 in *ortho*-dichlorobenzene (*o*-DCB) as the supporting electrolyte and by using a 2 mm diameter glassy carbon disk as the working electrode. Ferrocene (Fc) was added at the end of the experiments and used as an internal reference for measuring the potentials.

Figure 4 and Table 2 show the redox behavior of both $Pr_3N@C_{88}$ and $Ce_3N@C_{88}$, which was very similar to that of $Nd_3N@C_{88}$[14] and $Gd_3N@C_{88}$[15] reported recently. All of these EMFs show three reduction steps; the first is monoelectronic and reversible (peak to peak separation = 60 mV), the second is monoelectronic and quasi-reversible (peak to peak separation = 120–200 mV), and the third is less clearly defined and probably multielectronic. These compounds also show two reversible, monoelectronic oxidation steps. This behavior appears to be characteristic of the C_{88} EMFs. We note that $Ce_3N@C_{88}$, $Pr_3N@C_{88}$, and $Nd_3N@C_{88}$ also have very similar electrochemical HOMO–LUMO gaps, which is probably a consequence of their similar structures and the similar electronic properties of the encapsulated metals (see the electronegativity values of the three metals in Table 2).

As expected, $Nd_3N@C_{80}$ and $Pr_3N@C_{80}$ exhibited redox behavior that was comparable to that of previously described $Sc_3N@C_{80}$, $Er_3N@C_{80}$, $Y_3N@C_{80}$, $Dy_3N@C_{80}$, $Tm_3N@C_{80}$, and $Gd_3N@C_{80}$ (see Figures 5 and 6 and Table 3).[15,21–23]

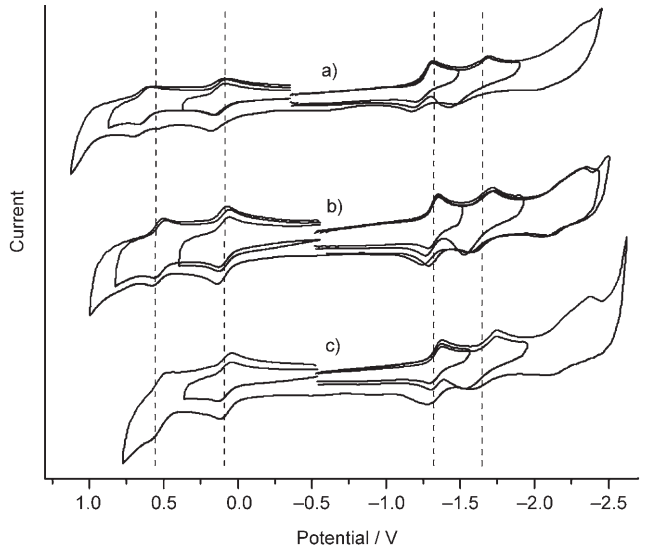

Figure 4. Cyclic voltammograms of a) $Ce_3N@C_{88}$, b) $Pr_3N@C_{88}$, and c) $Nd_3N@C_{88}$ in a 0.05 M solution of NBu_4PF_6 in *o*-DCB with ferrocene as the internal standard. The scan rate was 0.1 $V s^{-1}$.

Table 2. Half-wave potentials (vs. Fc^+/Fc) of the first reduction and oxidation steps of $Ce_3N@C_{88}$, $Pr_3N@C_{88}$, and $Nd_3N@C_{88}$.

	χ[a]	Redox potential		
		$E_{1/2,red(1)}$ [V]	$E_{1/2,ox(1)}$ [V]	ΔE_{gap} [V]
$Nd_3N@C_{88}$	1.14	−1.33	0.07	1.40
$Pr_3N@C_{88}$	1.13	−1.31	0.09	1.40
$Ce_3N@C_{88}$	1.12	−1.30	0.08	1.38

[a] Pauling electronegativity.[24]

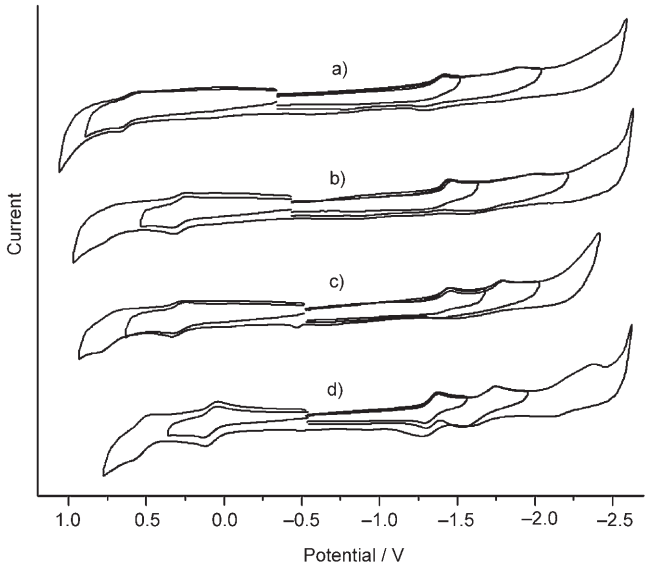

Figure 5. Cyclic voltammograms of a) $Nd_3N@C_{80}$, b) $Nd_3N@C_{84}$, c) $Nd_3N@C_{86}$, and d) $Nd_3N@C_{88}$ in a 0.05 M solution of NBu_4PF_6 in *o*-DCB with ferrocene as the internal standard. The scan rate was 0.1 $V s^{-1}$.

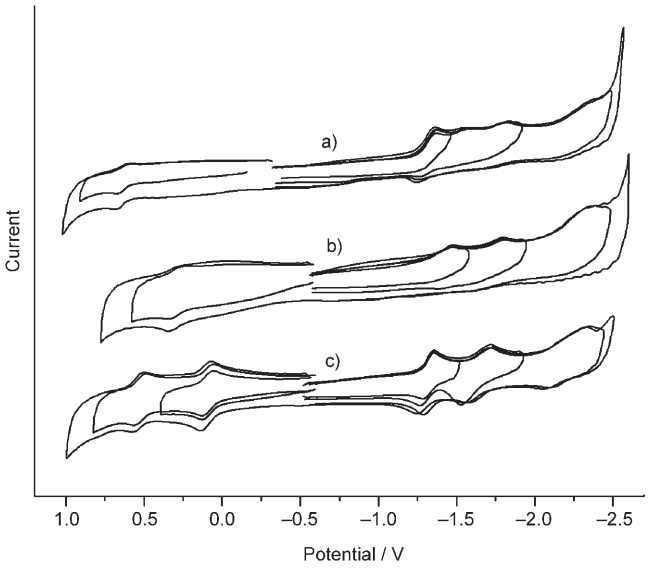

Figure 6. Cyclic voltammograms of a) $Pr_3N@C_{80}$, b) $Pr_3N@C_{86}$, and c) $Pr_3N@C_{88}$ in a 0.05 M solution of NBu_4PF_6 in *o*-DCB with ferrocene as the internal standard. The scan rate was 0.1 $V s^{-1}$.

Table 3. Cathodic peak potentials (vs. Fc^+/Fc) of the first reduction step and half-wave potentials of the other Nd- and Pr-based TNT EMFs isolated.

	$E_{p,red(1)}$ [V]	$E_{1/2,ox(1)}$ [V]	$E_{1/2,ox(1)}-E_{p,red(1)}$ [V]
$Nd_3N@C_{80}$	−1.42	0.63	2.05
$Pr_3N@C_{80}$	−1.41	0.59	2.00
$Nd_3N@C_{84}$	−1.44	0.31	1.75
$Nd_3N@C_{86}$	−1.46	0.36	1.82
$Pr_3N@C_{86}$	−1.48	0.31	1.78

One reversible oxidation step and at least two irreversible reduction steps were observed.

The first reduction process in Nd and Pr TNT EMFs was cathodically shifted compared with that of Sc TNT EMFs and was similar to that of Gd TNT EMFs, which is reasonable if the similar electronegativity values of Pr, Nd, and Gd (1.13–1.20) and the higher electronegativity value of Sc (1.36) are considered. $Nd_3N@C_{84}$ also showed at least two irreversible reduction steps and a reversible oxidation step, which were also previously observed for $Gd_3N@C_{84}$. Herein, we also report the electrochemical behavior of C_{86} TNT EMFs for the first time. Interestingly, the electrochemistry of $Nd_3N@C_{86}$ and $Pr_3N@C_{86}$ is qualitatively very similar to that of $Nd_3N@C_{84}$, $Nd_3N@C_{80}$, and $Pr_3N@C_{80}$ since these compounds also showed irreversible reduction and reversible oxidation behavior.

The electrochemical HOMO–LUMO gaps in these new EMF families follow the trends previously reported for the $Gd_3N@C_{2n}$ family.[15] A large gap was recorded for the C_{80} cage and a smaller one for the C_{88} cage. The cluster fullerenes encapsulated in C_{84} and C_{86} cages appear to have similar HOMO–LUMO gaps, which are intermediate between those of C_{80} and C_{88}.

Conclusion

The $Nd_3N@C_{2n}$ $(40 \le n \le 50)$, $Pr_3N@C_{2n}$ $(40 \le n \le 52)$, and $Ce_3N@C_{2n}$ $(43 \le n \le 53)$ EMF families were successfully synthesized, isolated, and characterized by mass spectroscopy, HPLC, UV/Vis-NIR spectroscopy, and cyclic voltammetry. To date, these compounds are the largest EMFs with the largest clusters encapsulated isolated. These three families of metallofullerenes all exhibited the same preferential templating of the C_{88} cage. When the ionic radii of the metal that formed the cluster was increased another tendency appeared, there was a progressive and significant increase in the yield of the $M_3N@C_{96}$ metallofullerene, which suggested that preferential templating of larger EMFs had occurred. The electronic properties of these new EMFs were studied and the results indicated that the size of the optical band gap decreased as the cage size increased. Metallofullerenes with the same cage size had similar band gaps and values of absorption, which suggested similar structures. The electrochemical properties of the three families were investigated by cyclic voltammetry and the results showed reversible reductions for the C_{88} cage compounds and irreversible reductions for smaller cages. The oxidation steps were easier for the larger cage compounds.

Experimental Section

High-purity graphite rods (6 mm diameter; purchased from POCO) were core-drilled (4 mm diameter) and packed with 3:1, 1:1, and 1:1 mixtures of graphite powder and CeO_2, Pr_6O_{11}, and Nd_2O_3, respectively. The rods were annealed at 1000 °C for 12 h and then vaporized by using an arc current of 85 A in a Krätschmer–Huffman arc reactor, under a mixture of ammonia (20 mbar) and helium (200 mbar). The soot from each packed rod was collected from the arc reactor and extracted with CS_2 in a sonicator for about two hours. After removal of the solvent, the crude mixtures were washed with diethyl ether and acetone until the washings were no longer colored. The solids were then dissolved in toluene and separated by HPLC (eluent: toluene) by using a semipreparative 10 mm × 250 mm Buckyprep-M column with a flow rate of 4 mL min^{-1}. MALDI-TOF mass spectrometry was carried out by using a Bruker Omni Flex spectrometer. For the EDS analysis, the samples were deposited on TEM grids and the spectra were recorded by using a HD-2000 STEM, equipped with an Oxford EDS system. Cyclic voltammetry was carried out in a one-compartment cell connected to a BAS 100B workstation in a 0.05 M solution of NBu_4PF_6 in *o*-DCB. UV/Vis-NIR spectra were obtained using a Perkin–Elmer Lambda 950 spectrophotometer.

Acknowledgements

Financial support from the National Science Foundation to A.J.A. and L.E. (Grant number CHE-0509989) is greatly appreciated. This research is based on work supported by the National Science Foundation while L.E. was working there. All opinions, findings, conclusions, or recommendations expressed herein are those of the authors and do not necessarily reflect the views of the National Science Foundation. The authors also gratefully thank Greg Becht and Professor Shiou-Jyh Hwu for their help in the annealing of the composite rods.

[1] S. Stevenson, G. Rice, T. Glass, K. Harich, F. Cromer, M. R. Jordan, J. Craft, E. Hajdu, R. Bible, M. M. Olmstead, K. Maitra, A. J. Fisher, A. L. Balch, H. C. Dorn, *Nature* **1999**, *401*, 55–57.
[2] L. Dunsch, M. Krause, J. Noack, P. Georgi, *J. Phys. Chem. Solids* **2004**, *65*, 309.
[3] S. Stevenson, H. M. Lee, M. M. Olmstead, C. Kozikowski, P. Stevenson, A. L. Balch, *Chem. Eur. J.* **2002**, *8*, 4528.
[4] M. Krause, J. Wong, L. Dunsch, *Chem. Eur. J.* **2005**, *11*, 706–711.
[5] S. Stevenson, J. P. Phillips, J. E. Reid, M. M. Olmstead, S. P. Rath, A. L. Balch, *Chem. Commun.* **2004**, 2814–2815.
[6] M. Krause, L. Dunsch, *Angew. Chem.* **2005**, *117*, 1581–1584; *Angew. Chem. Int. Ed.* **2005**, *44*, 1557–1560.
[7] M. Wolf, K.-H. Müller, Y. Skourski, D. Eckert, P. Georgi, M. Krause, L. Dunsch, *Angew. Chem.* **2005**, *117*, 3371–3374; *Angew. Chem. Int. Ed.* **2005**, *44*, 3306–3309.
[8] S. Yang, L. Dunsch, *J. Phys. Chem. B* **2005**, *109*, 12320–12328.
[9] T. Zuo, C. M. Beavers, J. C. Duchamp, A. Campbell, H. C. Dorn, M. M. Olmstead, A. L. Balch, *J. Am. Chem. Soc.* **2007**, *129*, 2035–2043.
[10] a) S. Stevenson, P. W. Fowler, T. Heine, J. C. Duchamp, G. Rice, T. Glass, K. Harich, E. Hajdu, R. Bible, H. C. Dorn, *Nature* **2000**, *408*, 427; b) M. M. Olmstead, A. de Bettencourt-Dias, J. C. Duchamp, S. Stevenson, H. C. Dorn, A. L. Balch, *J. Am. Chem. Soc.* **2000**, *122*, 12220–12226; c) S. Yang, M. Kalbac, A. Popov, L. Dunsch, *ChemPhysChem* **2006**, *7*, 1990–1995; d) S. Yang, A. A. Popov, L. Dunsch, *J. Phys. Chem. B* **2007**, *111*, 13659–13663; e) N. Chen, E. Zhang, C. Wang, *J. Phys. Chem. B* **2006**, *110*, 13322–13325; f) X. Wang, T. Zuo, M. M. Olmstead, J. C. Duchamp, T. E. Glass, F. Cromer, A. L. Balch, H. C. Dorn, *J. Am. Chem. Soc.* **2006**, *128*, 8884–8889; g) N. Chen, L. Fan, K. Tai, Y. Wu, C. Shu, X. Lu, C. Wang, *J. Phys. Chem. C* **2007**, 111, 11823–11828.
[11] M. Mikawa, H. Kato, M. Okumura, M. Narataki, Y. Kanazawa, N. Miwa, H. Shinohara, *Bioconjugate Chem.* **2001**, *12*, 510–514.
[12] H. Kato, Y. Kanazawa, M. Okumura, A. Taninaka, T. Yokawa, H. Shinohara, *J. Am. Chem. Soc.* **2003**, *125*, 4391–4397.
[13] J. M. Campanera, C. Bo, J. M. Poblet, *Angew. Chem.* **2005**, *117*, 7396–7399; *Angew. Chem. Int. Ed.* **2005**, *44*, 7230–7233.
[14] F. Melin, M. N. Chaur, S. Engmann, B. Elliott, A. Kumbhar, A. J. Athans, L. Echegoyen. *Angew. Chem.* **2007**, *119, 9190–9193; Angew. Chem. Int. Ed.* **2007**, 46, 9032–9035; *Angew. Chem. Int. Ed.* **2007**, *46*, 9032–9035.
[15] M. N. Chaur, F. Melin, B. Elliott, A. J. Athans, K. Walker, B. C. Holloway, L. Echegoyen, *J. Am. Chem. Soc.* **2007**, *129*, 14826–14829.
[16] P. W. Fowler, D. E. Manolopoulos in *An Atlas of Fullerenes*, Clarendon, Oxford, **1995**.
[17] a) A. A. Popov, L. Dunsch, *J. Am. Chem. Soc.* **2007**, *129*, 11835–11849; b) R. Valencia, A. Rodriguez-Fortea, J. M. Poblet, *Chem. Commun.* **2007**, 4161–4163.
[18] H. Shinohara, *Rep. Prog. Phys.* **2000**, *63*, 843–892.
[19] L. Dunsch, S. Yang, *Small* **2007**, *3*, 1298–1320.
[20] M. Krause, L. Dunsch, *ChemPhysChem* **2004**, 5, 1445.
[21] M. Krause, X. Liu, J. Wong, T. Pichler, M. Knupfer, L. Dunsch, *J. Phys. Chem. A* **2005**, *109*, 7088–7093.
[22] S. Yang, M. Zalibera, P. Rapta, L. Dunsch, *Chem. Eur. J.* **2006**, *12*, 7848–7855.
[23] C. M. Cardona, B. Elliott, L. Echegoyen, *J. Am. Chem. Soc.* **2006**, *128*, 6480–6485.
[24] *CRC Handbook of Chemistry and Physics*, 81st ed. (Ed.: D. R. Lide), CRC Press, New York City.

Received: January 9, 2008
Published online: April 9, 2008

